Level Set Methods for Geometric Inverse Problems in Linear Elasticity

Hend Ben Ameur *
hend.benameur@enit.rnu.tn

Martin Burger †
martin.burger@jku.at

Benjamin Hackl‡
hackl@sfb013.uni-linz.ac.at

July 17, 2003

Abstract

In this paper we investigate the regularization and numerical solution of geometric inverse problems related to linear elasticity with minimal assumptions on the geometry of the solution. In particular we consider the probably severely ill-posed reconstruction problem of a two-dimensional inclusion from a single boundary measurement.

In order to avoid parameterizations, which would introduce a-priori assumptions on the geometric structure of the solution, we employ the level set method for the numerical solution of the reconstruction problem. With this approach we construct an evolution of shapes with a normal velocity chosen in dependence of the shape derivative of the corresponding least-squares functional in order to guarantee its descent. Moreover, we analyze penalization by perimeter as a regularization method, based on recent results on the convergence of Neumann problems and a generalization of Golab's theorem.

The behavior of the level set method and of the regularization procedure in presence of noise are tested in several numerical examples. It turns out that reconstructions of good quality can be obtained only for simple shapes or for unreasonably small noise levels. However, it seems reasonable that the quality of reconstructions improves by using more than a single boundary measurement, which is an interesting topic for future research.

Keywords: Geometric Inverse Problems, Linear Elasticity, Level Set Method, Regularization.

AMS Subject Classification: 35R30, 49Q10, 74B05, 65J20

1 Introduction

This paper is devoted to the regularization and numerical solution of some geometric inverse problems in linear elasticity. We study the inverse problem of identifying interfaces or inclusions (with possibly multiple connected components) from boundary measurements. We develop a rather general approach to such geometric inverse problems in linear elasticity, where the normal component of the stress tensor satisfies a homogeneous boundary condition on the unknown geometry. The

*SFB, ENIT, LAMSIN, BP 51, 1002 Tunis Belbedere, Tunisia. This work was started during the visit to the JK university (Linz) as a research fellow 2002.

†Department of Mathematics, University of California, Los Angeles, 520 Portola Plaza, LA, CA 90095-1555, USA. On leave from: Johannes Kepler Universität Linz.

‡SBF F 013, Numerical and Symbolic Scientific Computing, Freistädterstr. 313, A-4040 Linz, Austria.

§This work was supported by the Austrian National Science Foundation (FWF) under the grant SFB F 013 / 08 and P13478-INF

boundary measurements in such applications are those of displacement on a part of the boundary where we have a boundary condition satisfied by the normal component of the stress tensor, too.

Geometric inverse problems, i.e., problems where the unknown is a geometric shape, are investigated for around three decades (cf. e.g. Dervieux and Palmerio [12], Kohn and Vogelius [24]) with respect to theoretical and numerical aspects. A standard approach for the solution of such problems consists in parameterizing the shape and applying regularization methods directly to the parameterization (cf. e.g. Hettlich and Rundell [17, 18, 19]). This approach suffers from the limitation that a lot of a-priori knowledge on the structure and topology of the solution shape has to been known in order to obtain convergent approximations. In particular, any parameterization does not allow a change in the number of components, and hence, a shape can be reconstructed if this number is known exactly. For the reasons described above, alternative approaches to the solution of shape reconstruction problems have been considered recently, such as the sampling methods (cf. Kirsch [23]) or the *level-set method* (cf. Santosa [42]). While the first one is based on properties of Dirichlet-Neumann type operators and therefore requires a large number of measurements, the level set method can be applied also in the case of a single Dirichlet-Neumann measurement, which we therefore consider in this paper. The level set approach was introduced by Osher and Sethian [37] for evolving geometries, with the original aim of deriving fast algorithms for a flame propagation problem. The basic idea is to represent a shape implicitly as the zero level set of a continuous function and to use the correspondence of geometric variations of the shape and the the solution of specific Hamilton-Jacobi equations for the level set function (cf. Section 4 for further details). Due to the implicit representation on an Eulerian grid, the level set approach does not introduce any a-priori assumptions on the geometry and therefore receives growing attention in the context of geometric inverse problems (cf. e.g. Burger [5, 6], Ito, Kunisch and Li [25], Ramananjaona et. al. [39, 40], Santosa et. al. [31, 42]). In this paper we shall investigate the application of level set methods in the context of elastic inclusion detection, which is a challenging problem both theoretically and numerically due to the Neumann condition on the boundary of the unknown shape.

By allowing rather general topology of the shape to be reconstructed, one also needs geometric regularization strategies independent of parameterizations. A frequently used approach is to add a multiple of the perimeter as a penalty to the least-squares functional. For problems that only dependent on the shape via its indicator function, this approach is equivalent to total variation regularization (cf. Rudin, Osher and Fatemi [41]) and can be analyzed in the standard framework developed by Acar and Vogel [1]. For a problem with Neumann boundary condition on the unknown interface, the least-squares functional is not lower semi-continuous with respect to the standard topologies for the indicator function and hence, a completely different approach has to be used. It turns out that the problem is lower-semicontinuous with respect to the Hausdorff-distance of shapes if an appropriate weak formulation (in Deny-Lions spaces) of the Neumann-problem is used. In this paper we will prove that perimeter penalization is indeed a convergent regularization method in this case, by using methods of geometric measure theory and novel results on the generalization of Golab's theorem (i.e., the lower semicontinuity of the perimeter with respect to the Hausdorff-distance metric). Moreover, we investigate the behavior of this regularization strategy in several numerical examples and compare it to a direct regularization by a level-set evolution, where the regularizing effect comes from an early termination of the evolution.

Throughout this paper we consider a homogeneous isotropic linear elastic material, in a domain $\mathcal{D} \subset \mathbb{R}^3$, assuming that there exists a surface $\Gamma \subset \mathcal{D}$ that separates the domain into two disjoint open sets $\mathcal{D}_1$ and $\mathcal{D}_2$, i.e.,

$$\overline{\mathcal{D}} = \overline{\mathcal{D}}_1 \cup \overline{\mathcal{D}}_2, \qquad \Gamma = \partial\mathcal{D}_1 \setminus \partial\mathcal{D} = \partial\mathcal{D}_2 \setminus \partial\mathcal{D}.$$

The linear elastic problem under consideration is specified by

$$\begin{array}{rcll} \operatorname{div} \sigma(u) & = & 0 & \text{in } \mathcal{D} \setminus \Gamma = \mathcal{D}_1 \cup \mathcal{D}_2 \\ \sigma(u) \, . \, n & = & 0 & \text{on } \Gamma \end{array} \tag{1.1}$$

supplemented by appropriate boundary conditions (specified below) on $\partial\Omega$, n denotes a normal vector to Γ. In the following we will use the convention that this normal vector is in the outward normal direction of $\mathcal{D}_1$. The vector u denotes the displacement and $\sigma(u)$ is the associated stress tensor, which is related via Hooke's law to the linearized strain tensor $\epsilon(u)$ via

$$\sigma = \lambda \,\mathrm{tr}\epsilon \, I + 2\mu \, \epsilon \,. \tag{1.2}$$

The linearized strain tensor $\epsilon(u)$ is given by

$$\epsilon_{ij}(u) = \frac{1}{2}\left(\frac{\partial u_i}{\partial x_j} + \frac{\partial u_j}{\partial x_i}\right),$$

tr denotes the trace of a matrix, and λ, μ are Lamé coefficients related to Young's modulus E and the Poisson ratio ν.

$$\mu = \frac{E}{2\,(1+\nu)} \qquad \lambda = \frac{E\nu}{(1-2\nu)\,(1+\nu)}\,.$$

The original identification process can be stated as:

Inverse Problem 3D: Identify the unknown shape Γ by applying some prescribed load g on $\Gamma_N \subset \partial\mathcal{D}$ and measuring the displacement induced by g on some part $\Gamma_M \subset \Gamma_N$ with Γ_M having a strictly positive measure.

We shall consider two two-dimensional cases derived from the three-dimensional problems for specific geometrical situations and special applied loads, the so-called *planar* and *anti-planar* cases. In these situations, uniqueness and stability results can be shown under rather general geometric assumptions (cf. Ben Ameur, Burger and Hackl [3]), which provides a clear theoretical basis. The full three-dimensional case shall be considered in future research.

This paper is organized as follows: In the remaining part of the introduction we reduce the full three-dimensional problem (1.1) to two-dimensional problems, and formulate the inverse problems that will be investigated further in the following sections. The regularization of the identification problem with minimal assumptions on the regularity of the shape is discussed in Section 2. In Section 3, we derive a level set method to solve the regularized problems, respectively as a regularizing evolution itself. Moreover, we discuss the numerical solution of the elasticity problem by the immersed interface method. We test the numerical behavior of the level set method and the regularization strategies in several numerical examples presented in Section 4, before we conclude and give an outlook to future work.

1.1 Planar and Anti-Planar Cases

We assume that $\mathcal{D} = \Omega \times \mathbb{R}$, where Ω is a bounded domain in $\mathbb{R}^2$, $\Omega = \Omega_1 \cup \Omega_2$ and $\Sigma = \partial\Omega_1 \cap \partial\Omega_2$. The different possible geometric situations are shown in Figure 1.

Furthermore we suppose that we apply a planar load g and that the displacement $u : \Omega \times \mathbb{R} \longrightarrow \mathbb{R}^3$ depends only on x_1 and x_2. We split the initial 3D problem (1.1) into two problems: A planar strain one, where we consider $u(x_1, x_2) = (u_1(x_1, x_2), u_2(x_1, x_2), 0)$, and an anti-planar problem depending only on the third component $u(x_1, x_2) = (0, 0, u_3(x_1, x_2))$.

In the planar strain case, we obtain a stress tensor σ satisfying $\sigma_{3,\ell} = \sigma_{\ell,3} = 0, \ell = 1, 2$. The choice of g with a third component equal to zero will allow us to obtain a two dimensional problem similar to the one corresponding to the plane stress case where $\sigma_{3,\ell} = \sigma_{l,\ell} = 0, l = 1, 2, 3$. We refer to both as "planar case" and rewrite (1.1) for the planar case as:

$$\begin{array}{rcll} \mathrm{div}\; \sigma(u) &=& 0 & \text{in } \Omega \setminus \Sigma \\ \sigma(u)\,.\,n &=& g & \text{on } \Gamma_N \\ \sigma(u)\,.\,n &=& 0 & \text{on } \Sigma \\ u &=& 0 & \text{on } \Gamma_D \end{array} \tag{1.3}$$

where $\{\Gamma_D, \Gamma_N\}$ is a partition of the boundary of Ω supporting Dirichlet and Neumann boundary conditions. The identification problem can then be stated as:

Inverse Problem, Planar Case: Identify the unknown interface Σ from a measurement of the displacement u on $\Gamma_M \subset \Gamma_N$ (with Γ_M having a strictly positive measure), where $u = (u_1, u_2)$

is the solution of (1.3) with the constitutive law (1.2).

Figure 1: Different situations

In the anti-planar case the original linear elasticity problem (1.1) reduces to a boundary value problem for a single Laplace equation:

$$\begin{array}{lcll} \mu\,\Delta\, u_3 & = & 0 & \text{in } \Omega\setminus\Sigma \\ \mu\frac{\partial u_3}{\partial n} & = & g & \text{on } \Gamma_N \\ \mu\frac{\partial u_3}{\partial n} & = & 0 & \text{on } \Sigma \\ u_3 & = & 0 & \text{on } \Gamma_D \end{array} \tag{1.4}$$

where μ is a Lamé constant.

For simplicity, we denote u_3 by u in (1.4) when the anti-planar case is concerned. The associated identification problem as can then be formulated as:

Inverse Problem, Anti-Planar Case: Identify the unknown interface Σ from a measurement of the vertical displacement u on $\Gamma_M \subset \Gamma_N$ (with Γ_M having a strictly positive measure), where u is the solution of (1.4).

1.2 Weak Formulations of the Direct Problem

In this section we introduce weak formulations of the direct problems (1.3) and (1.4), respectively, under minimal assumptions on the regularity of the interface Σ. In order to allow for general Hausdorff-measurable interfaces Σ, we use a framework in *Deny-Lions spaces*, recently used for the mathematical modeling and analysis of crack growth by Chambolle [8], Dal Maso and Toader [32] and Giacomini [16]. For smooth interfaces Σ, this solution concept coincides with the standard framework for weak solutions in Sobolev spaces.

In the following we assume that Σ is a compact subset of Ω with a finite number of connected components, which are measurable with respect to the Hausdorff measure $\mathcal{H}^1(\Sigma)$ (we refer to Federer [15] and Morel, Solimini [33] for details on the definition and properties of Hausdorff measures). Under such general condition a standard weak formulation is not suitable anymore, since one cannot define Sobolev spaces like $H^1(\Omega\setminus\Sigma)$ in a classical way. Therefore we introduce a generalization of Sobolev spaces for non smooth domains as follows: If A is an open subset of $\mathbb{R}^2$ (having in mind $A = \Omega\setminus\Sigma$, the *Deny-Lions space* $L^{1,2}(A)$ is defined by

$$L^{1,2}(A) := \{\ u \in W^{1,2}_{loc}(A) \mid \nabla u \in L^2(A;\mathbb{R}^2)\ \}.$$

Note that for a regular A, the *Deny-Lions space* coincides with the usual Sobolev space $H^1(A)$, but it is a strict superset for non regular sets. However, since we assume that Σ is a compact subset of Ω and $\partial\Omega$ is regular, each element in $L^{1,2}(\Omega\setminus\Sigma)$ is embedded in a local H^1-space in a neighborhood of the boundary so that we can define traces on $\partial\Omega$ in a standard way. Finally, we define the *Deny-Lions space* $L^{1,2}(A;\mathbb{R}^2)$ (cf. e.g. GIACOMINI [16] for further details).

$$L^{1,2}(A;\mathbb{R}^2) := \{\ u \in W^{1,2}_{loc}(A;\mathbb{R}^2) \mid \nabla u \in L^2(A;\mathbb{R}^{2\times 2})\ \}.$$

In the planar case, we specify the space of admissible vertical displacements as

$$\mathcal{U} := \{\ u \in L^{1,2}(\Omega \setminus \Sigma) \mid u|_{\Gamma_D} = 0\ \}. \tag{1.5}$$

The weak formulation of the anti-planar case consists in finding $u \in \mathcal{U}$ such that

$$a(u,v) := \int_{\Omega\setminus\Sigma} \nabla u.\nabla v\ dx = \int_{\Gamma_N} gv\ ds =: \langle G, v\rangle \qquad \forall\ v \in \mathcal{U}. \tag{1.6}$$

The solution of this problem is also the unique minimizer of the variational problem

$$a(u,u) - 2\langle G, u\rangle \to \min_{u\in\mathcal{U}}.$$

In the planar case, we can rewrite the variational problem in an analogous way, now with the vectorial *Deny-Lions space*

$$\mathcal{U} := \{\ u \in L^{1,2}(\Omega \setminus \Sigma;\mathbb{R}^2) \mid u|_{\Gamma_D} = 0\ \}. \tag{1.7}$$

and the variational form

$$a(u,v) := \int_{\Omega\setminus\Sigma} \sigma(u) : \epsilon(v)\ dx = \int_{\Gamma_N} g.v\ ds =: \langle G, v\rangle \qquad \forall\ v \in \mathcal{U},$$

with σ and ϵ defined as above, and $\sigma : \epsilon = \sum_{i,j} \sigma_{ij}\epsilon_{ij}$.

Finally we remark that for these weak formulations, existence and uniqueness of solutions for given interface Σ is guaranteed by the results in GIACOMINI [16]. In particular, the shape-to-output map $\Sigma \mapsto u|_{\Gamma_M}$ is well-defined, a fact that we shall use subsequently without further notice.

2 Geometric Regularization

Usually inclusion and interface identification problems are ill-posed. Even when for our problem class a local stability result was proofed in BEN AMEUR, BURGER AND HACKL [3] that might indicate the well-posedness of the inverse problems under consideration, these stability results, however, are valid only under strong additional assumptions on the shape, and only yield local and directional information. In particular, they provide no information about the stability with respect to general perturbations of the output data in $L^2(\Gamma_M)$, in whose norm we measure the error. The somehow minimal requirements for well-posedness in this output space would mean the existence of a solution to the least-squares problem

$$J_0(\Sigma) = \|u - \theta^\delta\|^2_{L^2(\Gamma_M)} \to \min_{\Sigma\in\mathcal{K}}$$

in some appropriate class of shapes $\mathcal{K}$ together with weak stability of the minimizer with respect to perturbations of the data θ^δ. As observed from the following example, weak stability in a general class of shapes does not hold:

Example 2.1. Let $\Omega = [0,1] \times [-1,1]$, $\Gamma_M = [0,1] \times \{1\}$ and define a sequence of interfaces Σ_n via

$$\Sigma_n = \{\ (x_1,x_2) \mid x_2 = \frac{1}{2}\sin n\pi x_1\ \}$$

with associated states u_n solving (1.4) and $f_n = u_n|_{\Gamma_M}$. Moreover we pose homogeneous Dirichlet conditions on $\Gamma_D = \{0,1\} \times (-1,1)$ and some Neumann boundary conditions g on $\Gamma_N = [0,1] \times$

$\{-1,1\}$, non-vanishing on Γ_M only. If ψ is the unique solution of $\Delta\psi = 0$ in Ω subject to this boundary conditions, then by the definition of u_n we obtain that

$$\int_\Omega |\nabla u_n|^2 \, dx + 2\int_{\Gamma_N} g u_n \, ds \leq \int_\Omega |\nabla \psi|^2 \, dx + 2\int_{\Gamma_N} g\psi \, ds := C$$

In particular we obtain for the integral over $S = (0,1) \times (\frac{1}{2}, 1)$

$$\int_S |\nabla u_n|^2 \, dx + 2\int_{\Gamma_N} g u_n \, ds \leq C.$$

The Poincaré inequality gives for functions in $H^1(S)$ with homogeneous Dirichlet values on $\{0,1\} \times (\frac{1}{2}, 1)$ that the first integral is an equivalent norm to the H^1-norm and if $\|g\|_{H^{-\frac{1}{2}}(\Gamma_M)}$ is sufficiently small, we obtain that

$$\int_S |\nabla u_n|^2 \, dx \leq \frac{C}{2}.$$

Thus, the restriction of u_n is uniformly bounded in $H^1(S)$ and due to the compactness of the trace operator from $H^1(S)$ to $L^2(\Gamma_M)$ there exists a subsequence of f_n converging to some f in $L^2(\Gamma_M)$, but the sequence Σ_n has no subsequence converging to a curve with finite Hausdorff measure $\mathcal{H}^1$. This example shows that without severe restrictions the problem is ill-posed even in any class of Σ piecewise in C^k (for any $k \in \mathbb{N}$) and $\mathcal{H}^1$-measurable, since the Σ_n constructed above are even analytic.

As usual for ill-posed problems we have to introduce a regularization approach in order to compute stable approximations of the solution in presence of data noise (cf. Engl, Hanke and Neubauer [13] for an overview on this subject), In the following parts we consider two different approaches to the regularization of (1.1), (1.2). The first one is a penalization approach motivated by the Mumford-Shah functional used frequently in image processing (cf. Morel and Solimini [33]), while the second consists in the early stopping of an evolution in artificial time, motivated by asymptotic regularization of inverse problems.

2.1 Penalization by Perimeter

A common approach to the stabilization of inverse interface problems is to add the perimeter (i.e., the Hausdorff measure $\mathcal{H}^1$) of Σ as a penalty to the output functional, i.e., to minimize

$$J_\alpha(\Sigma) = \frac{1}{2}\int_{\Gamma_M} |u - \theta^\delta|^2 \, ds \; + \; \alpha\mathcal{H}^1(\Sigma) \to \min_{\Sigma \in \mathcal{K}}, \tag{2.1}$$

where $\mathcal{K}$ denotes the class of compact subsets of Ω. Penalization by perimeter is well-analyzed in the context of the Mumford-Shah functional in image processing, where Σ represents the discontinuity set of the function u, whose L^2-distance to some given function is to be measured (see Morel and Solimini [33] for a comprehensive overview). Recently, this strategy has been used in the context of shape optimization or geometric inverse problems (cf. Ito, Kunisch and Li [21]). Problems with the analysis of this regularization strategy are caused in particular by the fact that the perimeter itself is not lower-semicontinuous in the class $\mathcal{K}$ with respect to the Hausdorff metric, which seems to be natural if the convergence of shapes is considered.

The lower semicontinuity on the subclass $\hat{\mathcal{K}}_1$ of simply connected, $\mathcal{H}^1$-measurable compact sets is provided by a classical result in geometric measure theory, called *Golab's Theorem* (cf. Morel and Solimini [33]). Due to recent results by Dal Maso and Toader [32] and in particular by Giacomini [16], the lower-semicontinuity of the perimeter is guaranteed on the more interesting class $\hat{\mathcal{K}}_m$ of $\mathcal{H}^1$-measurable compact sets with at most m connected components, which we shall use in our analysis below:

Theorem 2.2. *[32, Corollary 3.3] Let (Σ_n) be a sequence in $\hat{\mathcal{K}}_m$ converging to Σ in the Hausdorff metric. Then $\Sigma \in \hat{\mathcal{K}}_m$ and*

$$\mathcal{H}^1(\Sigma \cap \Omega) \leq \liminf_{n\to\infty} \mathcal{H}^1(\Sigma_n \cap \Omega).$$

Moreover, the results in these papers allow to deduce also the lower semicontinuity of the output functional and thus the analysis of this regularization strategy in a similar way to the analysis of standard Tikhonov regularization for nonlinear inverse problems (cf. Seidman and Vogel [43], Engl, Kunisch and Neubauer [14]), respectively to the analysis of the the so-called *total variation (TV) regularization* (cf. Rudin, Osher and Fatemi [41], Acer and Vogel [1]). The proof of the lower semicontinuity of the output-functional is the only property in this section for which we have to consider the two different cases of planar and anti-planar strain. We start with the anti-planar one, for which we use the results of Dal Maso and Toader [32]:

Proposition 2.3 (Lower Semicontinuity in the Anti-Planar Case). *The functional*

$$J_0 : \Sigma \mapsto \int_{\Gamma_M} |u - \theta|^2 \; ds$$

is lower semicontinuous on $\hat{\mathcal{K}}_m$ for arbitrary $\theta \in L^2(\Gamma_M)$, i.e. for any sequence (Σ_n) in $\hat{\mathcal{K}}_m$ converging to $\hat{\Sigma}$ in the Hausdorff metric, the solutions u_n respectively $\hat{u}$ of (1.5), (1.6) *with Σ replaced by Σ_n respectively $\hat{\Sigma}$, satisfy*

$$\int_{\Gamma_M} |\hat{u} - \theta|^2 \; ds \leq \liminf_{n\to\infty} \int_{\Gamma_M} |u_n - \theta|^2 \; ds.$$

Proof. Due to Dal Maso and Toader [32, Theorem 5.1], the gradients of the solutions u_n and $\hat{u}$ (extended by zero on Σ_n and $\hat{\Sigma}$ respectively) satisfy $\nabla u_n \to \nabla \hat{u}$ strongly in $L^2(\Omega; \mathbb{R}^2)$. Thus, for some open set U with $\Gamma_M \subset \partial U$, we obtain that $u_n \to u$ in $H^1(U)$ and thus, a standard trace theorem implies $u_n|_{\Gamma_M} \to \hat{u}|_{\Gamma_M}$ in $H^{\frac{1}{2}}(\Gamma_M) \hookrightarrow L^2(\Gamma_M)$. Together with the lower semicontinuity of the L^2-norm this implies the assertion. □

The proof in the planar case can be carried out in a completely analogous way, now using the results of Giacomini [16, in particular Lemma 6.1] and will thus be omitted here:

Proposition 2.4 (Lower Semicontinuity in the Planar Case). *The functional*

$$J_0 : \Sigma \mapsto \int_{\Gamma_M} |u - \theta|^2 \; ds$$

is lower semicontinuous on $\hat{\mathcal{K}}_m$ for arbitrary $\theta \in L^2(\Gamma_M; \mathbb{R}^2)$, i.e., for any sequence (Σ_n) in $\hat{\mathcal{K}}_m$ converging to $\hat{\Sigma}$ in the Hausdorff metric, the solutions u_n respectively $\hat{u}$ of (1.2),(1.7) *with Σ replaced by Σ_n respectively $\hat{\Sigma}$, satisfy*

$$\int_{\Gamma_M} |\hat{u} - \theta|^2 \; ds \leq \liminf_{n\to\infty} \int_{\Gamma_M} |u_n - \theta|^2 \; ds.$$

In the following we will not distinguish the planar and the anti-planar case, by considering data $f \in L^2(\Gamma_M)$ we will denote either scalar- or vector-valued functions. Moreover, for each Σ with some index, the function u, with the same index, will either denote the solution of (1.5),(1.6) or (1.2),(1.7), which we will use without further notice.

The first two results are concerned with the existence and (set-valued) stability of minimizers of (2.1) for $\alpha > 0$:

Proposition 2.5 (Existence of a Minimizer). *For any $\theta^\delta \in L^2(\Gamma_M)$ and any $\alpha > 0$ there exists a minimizer $\Sigma_\alpha^\delta \in \hat{\mathcal{K}}_m$ of* (2.1).

Proof. Let (Σ_n) be a minimizing sequence in $\hat{\mathcal{K}}_m$ (which exists since the functional is bounded below by zero), then due to the boundedness of Ω, there exists a convergent subsequence in the Hausdorff metric d_H with limit $\Sigma_\alpha^\delta \in \hat{\mathcal{K}}_m$. From the lower semicontinuity results in the preceding propositions we deduce that

$$\frac{1}{2}\int_{\Gamma_M} |u_\alpha^\delta - \theta^\delta|^2 \, ds + \alpha\mathcal{H}^1(\Sigma_\alpha^\delta) \le \frac{1}{2}\int_{\Gamma_M} |u_n - \theta^\delta|^2 \, ds + \alpha\mathcal{H}^1(\Sigma_n),$$

and thus, Σ_α^δ is a solution of (2.1). □

Proposition 2.6 (Stability). *Let $\alpha > 0$, let (θ_n) be a sequence in $L^2(\Gamma_M)$ converging to θ^δ and let (Σ_n) the associated sequence of minimizers in $\hat{\mathcal{K}}_m$ of (2.1) with data θ_n. Then, there exists a subsequence of (Σ_n) convergent in the Hausdorff-metric d_H and the limit of each convergent subsequence is a solution of (2.1) with data θ^δ.*

Proof. First of all, the existence of the minimizers $\Sigma_n \in \hat{\mathcal{K}}_m$ is guaranteed by Proposition 2.5. The existence of a convergent subsequence in the Hausdorff metric d_H follows from $\Sigma_n \subset \Omega$ and the boundedness of Ω. Now let Σ_n denote a converging subsequence with limit Σ_α^δ and let u_n, u_α^δ denote the associated sequence of states. Then, from the strong convergence $\theta_n \to \theta^\delta$ and the definition of u_n and Σ_n we deduce the inequality

$$\begin{aligned}
\frac{1}{2}\int_{\Gamma_M} |u_\alpha^\delta - \theta^\delta|^2 \, ds + \alpha\mathcal{H}^1(\Sigma_\alpha^\delta) \;&\le\; \liminf_{n\to\infty} \frac{1}{2}\int_{\Gamma_M} |u_n - \theta^\delta|^2 \, ds + \alpha\mathcal{H}^1(\Sigma_n)\\
&\le\; \liminf_{n\to\infty} \frac{1}{2}\int_{\Gamma_M} |u_n - \theta_n|^2 \, ds + \alpha\mathcal{H}^1(\Sigma_n)\\
&\le\; \lim_{n\to\infty} \frac{1}{2}\int_{\Gamma_M} |u - \theta_n|^2 \, ds + \alpha\mathcal{H}^1(\Sigma)\\
&\le\; \frac{1}{2}\int_{\Gamma_M} |u - \theta^\delta|^2 \, ds + \alpha\mathcal{H}^1(\Sigma)
\end{aligned}$$

for any $\Sigma \in \hat{\mathcal{K}}_m$ with associated state u. Hence, the limit Σ_α^δ is also a solution of problem (2.1). □

Now, we are able to prove the main result of this section, namely that penalization by perimeter is a convergent regularization method in $\hat{\mathcal{K}}_m$ equipped with the Hausdorff metric d_H:

Theorem 2.7 (Convergence). *Suppose that there exists $\Sigma^* \in \hat{\mathcal{K}}_m$ such that the according solution u^* of (1.5),(1.6) or (1.2),(1.7), respectively, satisfies $u^*|_{\Gamma_M} = \theta$. Let θ^δ be such that*

$$\|u^* - \theta^\delta\|_{L_2(\Gamma_M)} \;\le\; \delta \tag{2.2}$$

holds and let α be chosen such that

$$\alpha \to 0, \qquad \frac{\delta^2}{\alpha} \to 0 \qquad \text{as } \delta \to 0.$$

Then, for the according solutions Σ_α^δ of (2.1), there exists a subsequence convergent in the Hausdorff metric d_H and the limit $\hat{\Sigma}$ of every convergent sequence is a minimum-perimeter solution of the identification problem, i.e. the associated displacement $\hat{u}$ satisfies $\hat{u}|_{\Gamma_M} = \theta$ and for all other solutions Σ, we have that

$$\mathcal{H}^1(\hat{\Sigma}) \le \mathcal{H}^1(\Sigma).$$

Proof. Again by boundedness, there exists a subsequence $(\Sigma_n) := (\Sigma_{\alpha_n}^{\delta_n})$ converging in the Hausdorff metric d_H. Now let (Σ_n) be such a convergent subsequence with limit $\hat{\Sigma}$. By the definition of Σ_n we obtain by comparison with Σ^* that

$$\frac{1}{2}\int_{\Gamma_M} |u_n - \theta^{\delta_n}|^2 \, ds + \alpha_n\mathcal{H}^1(\Sigma_n) \le \frac{1}{2}\int_{\Gamma_M} |\theta - \theta^{\delta_n}|^2 \, ds + \alpha_n\mathcal{H}^1(\Sigma^*) = \frac{\delta_n^2}{2} + \alpha_n\mathcal{H}^1(\Sigma^*).$$

Division by α_n and the assumption $\frac{\delta_n^2}{\alpha_n} \to 0$ shows that $\mathcal{H}^1(\Sigma_n)$ is uniformly bounded and the lower semicontinuity of the Hausdorff measure yields $\mathcal{H}^1(\hat{\Sigma}) \leq \mathcal{H}^1(\Sigma^*)$. Moreover, as $\delta_n \to 0$, we obtain that

$$\frac{1}{2}\int_{\Gamma_M} |\hat{u} - \theta|^2 \, ds \leq \liminf_{n\to\infty} \frac{1}{2}\int_{\Gamma_M} |u_n - \theta^{\delta_n}|^2 \, ds \leq \liminf_{n\to\infty} \frac{\delta_n^2}{2} + \alpha_n \mathcal{H}^1(\Sigma^*) = 0.$$

Thus, $\hat{\Sigma}$ is a solution of the identification problem and since the solution Σ^* is arbitrary, it is also a minimum-perimeter solution. □

We finally remark that we obtain strong convergence by a standard principle, if the minimum-perimeter solution is unique. In particular this would be guaranteed by an identifiability result in the class $\hat{\mathcal{K}}_m$, but so far we can only give such a result for disjoint unions of smooth curves (cf. Ben Ameur, Burger, Hackl [3]).

3 Numerical Solution

In this section we discuss a level set approach to the solution of the identification problem, respectively to the optimization problem (2.1) obtained from penalization by perimeter. Furthermore we discuss the solution of the arising Hamilton-Jacobi equation as well as the solution of the elliptic problem with moving interface.

3.1 Level Set Methods

The level set approach to geometric motion has been introduced by Osher and Sethian [37]. Its main idea is to represent an evolving front as the zero level set of a continuous function, i.e.

$$\Sigma(t) = \{ \ x \in \Omega \mid \phi(x,t) = 0 \ \}.$$

A weak formulation of geometric motion with normal speed V_n is given by the Hamilton-Jacobi equation

$$\frac{\partial \phi}{\partial t} + V_n |\nabla \phi| = 0 \qquad \text{in } \mathbb{R}^d \times \mathbb{R}^+ , \tag{3.1}$$

in the sense that a viscosity solution for this Hamilton-Jacobi equation (3.1) has to be computed. We refer to the monograph by Lions [30] and the paper by Crandall et al. [10] for details on the notion of viscosity solution. The function V_n in the Hamilton-Jacobi equation (3.1) is an extension of the velocity from the front to the whole $\mathbb{R}^N$ (or subset of $\mathbb{R}^N$ being the computational domain and including the interface).

The basic idea of level set methods for inverse and optimization problems (cf. Burger [5], Ito, Kunisch and Li [21], Santosa et al. [36, 42] and Ramananjaona et al. [39, 40]) is to choose the velocity in such a way that a decrease of the objective functional is achieved, which resembles the classical speed method in shape optimization (cf. Murat and Simon [34], Sokolowski and Zolesio [46]), but the weak formulation via the level set method allows for more general evolutions and in particular for topological changes such as splitting or merging of domains. We restrict our attention again to the anti-planar case, noting that analogous reasoning is possible for the planar case.

In the following we discuss the construction of level set methods based on the original sharp interface model for the state equation. The basic tool for the choice of the velocity is the *shape derivative* in direction of a normal velocity V_n (cf. Sokolowski and Zolesio [46] and Delfour and Zolesio [11]), which coincides with the time derivative of the objective functional J_α, when the shape is evolved according to the geometric motion defined by (3.1). For the detailed computation of shape derivatives we refer to Ben Ameur, Burger, Hackl [3], here we briefly present the result in the anti-planar case, the planar case can be treated in an analogous way. The time derivative of $J(\Sigma(t))$ under a geometric motion with normal velocity is given by

$$\frac{d}{dt} J_\alpha(\Sigma(t)) = \int_{\Gamma_M} (u - \theta^\delta)\; u' \, ds \;+\; \alpha \int_{\Sigma} V_n \kappa \, d\mathcal{H}^1, \tag{3.2}$$

where κ denotes the mean curvature of Σ, and u' is the solution of

$$\begin{array}{lcll} \Delta u' & = & 0 & \text{in } \Omega \setminus \Sigma \\ \frac{\partial u'}{\partial n} & = & 0 & \text{on } \Gamma_N \\ \frac{\partial u'}{\partial n} & = & -\mathrm{div}_T (V_n \nabla_T\, u) & \text{on } \Sigma \\ u' & = & \frac{\partial u}{\partial n} V_n & \text{on } \Gamma_D \end{array} \tag{3.3}$$

Introducing the adjoint problem

$$\begin{array}{lcll} \Delta w & = & 0 \text{ in } \Omega \setminus \Sigma & \\ \frac{\partial w}{\partial n} & = & \chi_{\Gamma_M} (u - \theta^\delta) & \text{on } \Gamma_N \\ \frac{\partial w}{\partial n} & = & 0 & \text{on } \Sigma \\ w & = & 0 & \text{on } \Gamma_D \end{array} \tag{3.4}$$

where χ_{Γ_M} is the indicator function of Γ_M, we can deduce a simple formula for the derivative of J_α:

$$\frac{d}{dt} J_\alpha(\Sigma(t)) \; = \int_\Sigma (-\nabla_T u . \nabla_T w + \alpha\kappa)\, V_n \; ds \tag{3.5}$$

The Hadamard speed method consists in choosing the velocity V_n such that a steepest descent (or a gradient flow) is achieved with respect to an appropriate norm for the velocity V_n (cf. Sokolowski and Zolesio [46], Burger [6]). As discussed in Burger [6] we have several possibilities to choose the velocity via the speed method, in particular we consider the steepest in $L^2(\Sigma(t))$ and in $H^{\frac{1}{2}}(\Sigma(t))$. For the L^2-case we obtain the velocity on $\Sigma(t)$ as

$$V_n = [\nabla u . \nabla w] - \alpha\kappa := V_n^0 - \alpha\kappa, \qquad \text{on } \Sigma(t),$$

which corresponds to the classical version of the speed method and the standard approach for level set methods in inverse obstacle problems. Since preliminary numerical experiments indicate that this standard approach fails for the problem we consider, we use the gradient flow in the norm of $H^{\frac{1}{2}}(\Sigma(t))$, which lead to reasonable results in Burger [6]. In the case of the $H^{\frac{1}{2}}$-norm, we have additional smoothing of the velocity V_n via

$$\begin{array}{lcll} \Delta \psi_{V_n} & = & 0 & \text{in } \Omega \setminus \Sigma \\ \frac{\partial \psi_{V_n}}{\partial n} & = & 0 & \text{on } \Gamma_N \\ \frac{\partial \psi_{V_n}}{\partial n} & = & [\nabla u . \nabla w] - \alpha\kappa & \text{on } \Sigma(t) \\ \psi_{V_n} & = & 0 & \text{on } \Gamma_D \end{array} \tag{3.6}$$

and then obtain the velocity as the trace $V_n = \psi_{V_n}$ on $\Sigma(t)$. Since ψ_{V_n} is an extension of V_n to the whole domain Ω, we can use it directly as an extension velocity for the level set method, so that the resulting evolution equation is given by

$$\frac{\partial \phi}{\partial t} + \psi_{V_n} |\nabla \phi| = 0.$$

Since the normal jump has a meaning only on $\Sigma(t)$ we need to compute an extension velocity at least in a neighborhood of $\Sigma(t)$, which can be realized e.g. by solving a stationary Hamilton-Jacobi equation as in Adalseinsson and Sethian [2]. Alternatively, we could also perform a strategy as for the $H^{\frac{1}{2}}$-case and solve the problem (3.6) with Dirichlet data V_n^0. Extensions of th curvature to the whole domain can be obtained as (cf. OSHER AND SETHAIN [37]) $\kappa = \text{ div } \left(\frac{\nabla\phi}{|\nabla\phi|}\right)$, which finally leads to the level set evolution (with V^0 being an appropriate extension of V_n^0)

$$\frac{\partial \phi}{\partial t} + V^0|\nabla\phi| - \alpha|\nabla\phi| \text{ div } \left(\frac{\nabla\phi}{|\nabla\phi|}\right) = 0.$$

For $\alpha = 0$, this evolution is a first-order Hamilton-Jacobi equation with a non local term caused by the dependence of V^0 on the zero level set; for $\alpha > 0$ the evolution is of second order.

We want to mention that in the case $\alpha = 0$, the associated least-squares problem is ill-posed, but we may still consider the speed method as an evolutive regularization method. As for any regularizing evolution for ill-posed problems in presence of noise, an appropriate stopping criterion is needed relating the time T_* at which the evolution is terminated with the noise level δ in (2.2). By analogy to the method of asymptotic regularization (cf. TAUTENHAN [47]) and to a regularizing level set evolution for a class of shape reconstruction problems (cf. BURGER [5] where a rigorous analysis has been carried out), we propose to use the *discrepancy principle*, choosing T_* via

$$T_*(\delta, \theta^\delta) := \inf\{\ t \in \mathbb{R}_+ \mid \|u(t)|_{\Gamma_M} - \theta^\delta\|_{L^2(\Gamma_M)} \leq \tau\delta\ \}$$

for appropriate (fixed) parameter $\tau > 1$. We shall compare the results obtained with this regularization approach, which we call *terminated speed method*, to the ones obtained with penalization by perimeter in the next section.

3.2 Solving the Hamilton-Jacobi equation (3.1)

For solving the Hamilton-Jacobi equation (3.1) numerically, we merely use well-known schemes. There is a vast literature on numerical solvers for Hamilton-Jacobi equations (e.g. see see OSHER ET AL. [35, 38], JIANG AND PENG [22]) being based on the idea of essentially non-oscillatory schemes.

In all our numerical tests we used a 5^{th} order WENO scheme to discretize the spatial part of the Hamilton-Jacobi equation and an explicite Runge-Kutta scheme of 3^{rd} order to solve the time part of the Hamilton-Jacobi equation (see JIANG AND PENG [22]). Due to the finite domain we added homogeneous Neumann Boundary conditions to the Hamilton-Jacobi equation. The influence of this boundary condition can be ignored however, since the inclusions do not touch the boundary in the cases under consideration.

The explicit time integration of the Hamilton-Jacobi equation requires to fulfill the CFL condition to maintain a stable Hamilton-Jacobi solver. This means that the time step Δt is restricted by

$$\Delta t \ \leq \ c\frac{h}{\|\psi_{V_n}\|_{L_\infty(\Omega)}},$$

with a constant $c < 1$, where h denotes the mesh size. In all our numerical tests we chose $c = 0.8$, which produced reasonable results.

According to theory the calculated velocity V_n should result into a descent of the objective $J_\alpha(\Sigma)$ (equation (2.1)). By using the CFL condition to determine the time step in the Hamilton-Jacobi solver we observed that this might also result in an increase of the objective. This may caused by the fact that the CFL-time step is too large or due to a poor approximation of the solution of the PDE (1.4) or the adjoint PDE (3.4). Note that it may happen that one obtains a high approximation error for the PDE (1.4) and the adjoint PDE (3.4) because of a poor approximation of the normal to the zero level set, which occurs if the level set function is highly oscillating close to the zero level set. In this case a reinitialization of the level set function may help.

Obviously, the increase of the objective $J_\alpha(\Sigma)$ during the iteration is not desirable in an optimization context and hence, additionally to the CFL restriction, we restricted the time step Δt such that a decrease in the objective is guaranteed. This was realized by implementing a simple line-search (bisection), up to some minimal step size (at most 10 bisections), which nonetheless caused some increases in the objective. Due to the possible poor approximation of the normal at the zero level set we additionally reinitialized the level set function to the signed distance function when the step size reached its minimum. Nonetheless, the average behavior of the objective $J_\alpha(\Sigma)$ is decreasing so that the remaining increases in the objective can be accepted.

Finally we want to remark on the termination criteria for the perimeter regularization. Usually one would use a standard termination criteria from optimization for the regularized problem, e.g., terminate when

$$d_H(\Sigma_{i+1}, \Sigma_i) \leq \epsilon$$

where ϵ is a small positive number. Our calculation of the Hausdorff distance has accuracy $d_H = O(h)$, so it is impossible to choose ϵ very small ($\epsilon < h$). On the other hand the choice $\epsilon \geq h$ would cause a too early termination of the algorithm. Hence, we chose to terminate according to a proper chosen number of iterations such that by experience the Hausdorff distance d_H did not change.

3.3 Solving the Elliptic PDE (1.4)

One of the major issues in the numerical solution of inverse obstacle problems, crack identification, shape optimization and also moving boundary problems is the type of discretization used for the underlying elliptic or parabolic partial differential equations, in particular the question whether the mesh should be changed during the optimization or evolution process or not. Mainly three different approaches to this problem can be found in literature, namely finite element method, fictitious domain methods, and the immersed interface method. For our numerical simulations, we used the latter, mainly because of the theoretically well studied properties, the fixed grid for all time (optimization) steps and due to the available Fortran sources for the IIM solver, provided by Zhilin Li. One further advantage of the IIM in our application is that the finite difference grid can also be used to discretize the Hamilton-Jacobi equation (3.1).

All standard finite element discretization of the PDE (1.4) face one problem in the level-set approach, namely the need of two different meshes, a triangular one for the elliptic equation and a rectangular finite difference grid for the Hamilton-Jacobi equation. This is mainly because almost all well analyzed discretization schemes for the Hamilton-Jacobi equation are based on finite difference discretization. It is usually not desirable to map quantities from one grid to another, which may introduce a loss in accuracy and further numerical instabilities. However, we want to remark that numerical tests with a finite-element based *fictitious domain method* lead to similar results as for the *IIM*.

The *immersed interface method* was originally developed to treat elliptic interface problems with a finite difference discretization. It is proved to be of optimal accuracy, furthermore the interface and the finite difference grid are independent. For more details see Li et al. [26, 27, 20, 29]. The IIM seems to be quite well suited for interface identification problems because the finite difference grid for the PDE can be fixed once and for ever (no remeshing). Using a similar trick as in the *fictitious domain method* it is also possible to treat inclusion or boundary identification problems with the IIM. This procedure is described in more detail in the following Section 3.3.1.

3.3.1 Immersed Interface Method for Inclusions

Originally the IIM was developed to treat interface problems with a finite difference discretization (see Li et al. [26, 20, 29]). To solve also inclusion or boundary problems (1.4) with the IIM we have to transform the inclusion or boundary problem to an interface problem. We do this transformation along the suggestions of Li et al. [27, 21] for the inclusion problem (1.4) only.

First we extend the solution of the inclusion problem (1.4) to the inclusion Ω_- such that

$$\Delta u = 0 \qquad \text{in} \qquad \Omega_- .$$

For this sake we can either use the extension in $H^1(\Omega)$, i.e. $[u]|_\Sigma := u_+ - u_- |_\Sigma = 0$, or require the jump of the normal derivative $\left[\frac{\partial u}{\partial n}\right]|_\Sigma$ at the inclusion to be zero. In this way we get naturally the following equivalent formulations of the inclusion problem (1.4).

$$\begin{array}{lll} \Delta u &= 0 & \text{in}\,\Omega^+ \\ u|_{\Gamma_D} &= 0 & \\ \frac{\partial u}{\partial n}|_{\Gamma_N} &= f & \\ \frac{\partial u}{\partial n}|_{\Sigma} &= 0 & \end{array} \quad \Leftrightarrow \quad \begin{array}{lll} \Delta u &= 0 & \text{in}\,\Omega\setminus\Sigma \\ u|_{\Gamma_D} &= g & \\ \frac{\partial u}{\partial n}|_{\Gamma_N} &= f & \\ [u]|_{\Sigma} &= 0 & \\ [\frac{\partial u}{\partial n}]|_{\Sigma} &= -\frac{\partial u}{\partial n_-} & \end{array} \quad \Leftrightarrow \quad \begin{array}{lll} \Delta u &= 0 & \text{in}\,\Omega\setminus\Sigma \\ u|_{\Gamma_D} &= g & \\ \frac{\partial u}{\partial n}|_{\Gamma_N} &= f & \\ [u]|_{\Sigma} &= u_+ & \\ [\frac{\partial u}{\partial n}]|_{\Sigma} &= 0 & \end{array} \tag{3.7}$$

Solving any of these equivalent formulations (if $\text{meas}(\Gamma_D) > 0$) is a well posed problem (in particular unique). The last two formulations are interface problems in a fixed point form.

Introducing a new variable w for either $-\frac{\partial u}{\partial n_-}|_\Sigma$ or $u_+|_\Sigma$ we get a Saddle point form that is equivalent to the original PDE (3.7)

$$\begin{array}{lll} \Delta u &= 0 & \text{in}\,\Omega\setminus\Sigma \\ u|_{\Gamma_D} &= g & \\ \frac{\partial u}{\partial n}|_{\Gamma_N} &= f & \\ [u]|_{\Sigma} &= 0 & \\ [\frac{\partial u}{\partial n}]|_{\Sigma} - w &= 0 & \\ \frac{\partial u}{\partial n_+}|_{\Sigma} &= 0 & \end{array} \quad \Leftrightarrow \quad \begin{array}{lll} \Delta u &= 0 & \text{in}\,\Omega\setminus\Sigma \\ u|_{\Gamma_D} &= g & \\ \frac{\partial u}{\partial n}|_{\Gamma_N} &= f & \\ [u]|_{\Sigma} - w &= & \\ [\frac{\partial u}{\partial n}]|_{\Sigma} &= 0 & \\ u_-|_{\Sigma} &= 0 & \end{array}$$

Note that the restriction $\frac{\partial u}{\partial n_+}|_\Sigma = 0$ and $u_-|_\Sigma = 0$ has to be done in $H^{-\frac{1}{2}}(\Sigma)$ and $H^{\frac{1}{2}}(\Sigma)$.

Next we discretize this system according to the IIM, i.e., the interface problem becomes

$$Au + Bw = F\,,$$

where A is the discretization of the Laplacian (e.g. 5-point stencil) and B, F is calculated due to the rules for IIM (see LI [27]). Like in the work of ITO, LI AND KUNISCH [21, 27] we discretize the restriction $\frac{\partial u}{\partial n_+}|_\Sigma, u_+|_\Sigma = 0$ using some properties of the IIM resulting into

$$Cu + Dw = G\,,$$

where C, D, G are matrices respectively vectors obtained from the immersed interface discretization. One requirement we do not meet, using this discretization of the restriction, is that we discretize the restriction in $L_2(\Sigma)$ (more accurate $l_2(\Sigma)$) instead of $H^{\frac{1}{2}}(\Sigma)$ or $H^{-\frac{1}{2}}(\Sigma)$. Due to tests done by LI [27] this seems not to have much influence and so we nonetheless use this discretization.

Finally we can eliminate the variable u by using the inverse of the operator A. Computationally the application of this inversion can be realized very efficiently by fast Poison solvers. When we substitute u into the equation for the restriction we end up with a smaller Schur complement equation

$$(D - CA^{-1}B)w = G - CA^{-1}F\,.$$

We solve this equation by the generalized minimum residual method (GMRES). According to LI [27] the number of iterations to solve this equation with the GMRES is independent of the mesh size (which we also observed numerically for the inclusion problem) and so we obtain an efficient method to solve the inclusion problem (3.7). Clearly some analysis is missing, especially concerning the stability of the discrete system, i.e., whether the Schur complement can be inverted stable and independent of the mesh size, or not.

Remark 1.

- *The operators A, A^{-1}, B, C, D are never calculated explicitely. Only their applications are needed, which makes computations efficient.*
- *For certain shapes, especially shapes with very high curvatures (locally), we observed that the solution to the discrete system do not fit to the real solution very well. Probably this is either due to an instable calculation of the operators B, C, D and vectors F, G according to the IIM or due to a not properly converging GMRES procedure caused by the wrong space for the restriction equation ($l_2(\Sigma)$ instead of $H^{\frac{1}{2}}(\Sigma)$, $H^{-\frac{1}{2}}(\Sigma)$).*

- *In our calculations we used the reformulated PDE* (3.7) *with the Dirichlet restriction* $u_-|_\Sigma = 0$.

4 Numerical Results

In the following we shall report on some numerical experiments carried out with the methods described in the previous section to test the newly developed theory about the perimeter regularization as well as the proposed terminated speed method.

We restrict ourselves to the anti-planar case (1.4), because numerical tools are available for this case, similar results can be expected for the planar case. All performed tests are done with the same test configuration, i.e. we did all calculations on a square domain $\Omega = [-1,1] \times [-1,1]$ with fixed boundary conditions. Only the inclusion Ω_- and the corresponding measurements vary from example to example. The geometric configuration, the boundary conditions and the problem specification are given in the following picture:

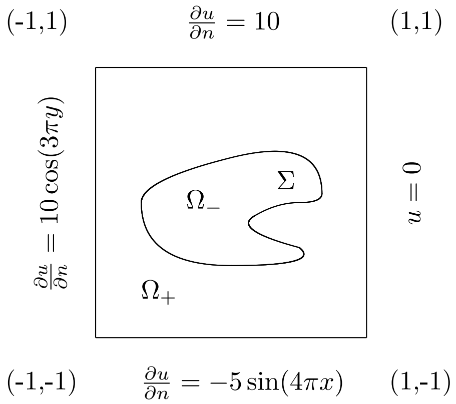

$$\begin{aligned} \Delta u &= 0 \quad \text{in}\, \Omega_+ \\ u|_{\Gamma_D} &= 0 \\ \frac{\partial u}{\partial n}|_{\Gamma_N} &= h \\ \frac{\partial u}{\partial n}|_{\Sigma} &= 0 \end{aligned}$$

Measurements:

$$\theta^\delta \ = \ u|_{\Gamma_N} \,\text{in}\, L_2(\Gamma_N)$$

For the starting value ϕ_0 of the Hamilton-Jacobi equation (3.1) we chose for all test examples $\phi_0 = x^2 + y^2 - 0.3^2$, i.e. a level set function having as zero level line a circle with center $(0,0)$ and radius 0.3.

To avoid inverse crimes (see comments by Colton and Kress [9, p. 133]) we calculated our measurements on a very fine grid (e.g. 2049x2049), having no grid points in common with the one later used for the numerical solutions of the inverse problem. These artificial measurements were projected by linear interpolation to the grid for the inverse problem.

The stability and convergence of the terminated speed method as well as the perimeter regularization was tested by perturbing the measurements with some artificial noise (of levels $\delta = 5, 3, 1, 0.8, 0.5, 0.3, 0.1\,\%$). We generated this noise using Gaussian random values for every measurement point. Then we scaled this artificially produced noise by its $L_2(\Gamma_N)$-norm, which was added, scaled by its (normalized) noise level $\frac{\delta \|u\|_{\Gamma_N}}{100}$, to the (exact) measurements.

Remark 2. *Even for exact measurements our solver faces noisy data. This is due to the (coarse) discretization of the PDE. For the discretization we chose we expect approximately an additional noise of* $\sim 0.1\%$.

Terminated Speed Method: The discrepancy principle was chosen to terminate with $\tau = 2$, i.e. solve the Hamilton-Jacobi equation (3.1) as long as $\|u(T) - \theta^\delta\|_{L_2(\Gamma_M)} \ \geq \ 2\delta \|\theta^\delta\|_{L_2(\Gamma_N)}$.

Perimeter Regularization: For the perimeter regularization we chose the penalization parameter α to be proportional to the noise level, i.e., $\alpha = c\delta$. According to the theory developed in Section 2.1 this is a stable and converging method. Since we do not have a useful rule how to chose the constant c, we used $c = 5$ for all our test examples (corresponding merely to the scaling of the problem).

For almost all tests we plotted the Hausdorff distance $d_H(\Sigma_\alpha^\delta, \Sigma^*)$ versus the the noise level δ (in logarithmic scale). Additional to the Hausdorff distance which is a very strong measure to compare the quality of several identification results, we also plotted the L_1 distance, i.e.

$$d_1(\Sigma_\alpha^\delta, \Sigma^*) = \int_\Omega |\chi_{\{\hat{\phi}_\alpha^\delta \leq 0\}} - \chi_{\{\hat{\phi} \leq 0\}}| \,\mathrm{dx}\,,$$

versus the noise level δ (logarithmic scale).

For inverse problems there are usually no benchmark examples available. Hence we chose our test examples such that they are somehow representative for this class of problems, not too simple and challenging for the algorithm.

4.1 Ellipse

For the first test example the inclusion is an ellipse with respect ratio 5/3.

$$\Sigma^* = \left\{ (x,y) \,|\, \left(\frac{x}{0.5}\right)^2 + \left(\frac{y-0.1}{0.3}\right)^2 = 1 \right\}$$

This is probably the simplest example so we can expect that the algorithm performs well. For the discretization of the PDE (3.7) and the Hamilton-Jacobi equation (3.1) we chose a 257x257 grid. In Figure 2 we present the calculated inclusions for the noise levels $\delta = 5, 1, 0.5, 0.1\,\%$ as well

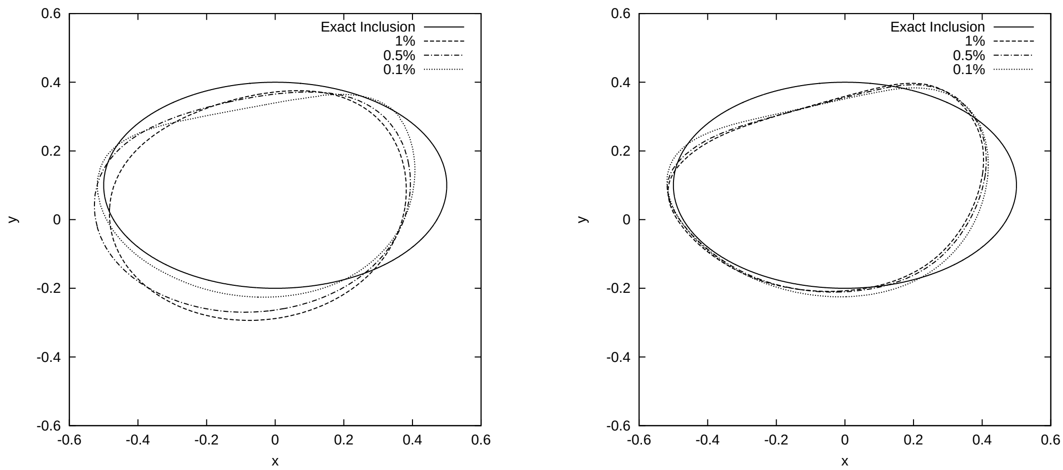

(a) Terminated Speed Method (b) Perimeter Regularization

Figure 2: Ellipse: Identified inclusion for $\delta = 1, 0.5, 0.1\%$

as the exact shape for both the terminated speed method and the perimeter regularization. One observes that the reconstructed inclusion approaches the exact inclusion with decreasing noise level, as predicted by theory. Only parts of the inclusion close to the Dirichlet boundary and close to the Neumann boundary with constant load are of poor quality. For the part close to the Dirichlet boundary this is not unexpected, since here we have no measurements and so the objective will not be very sensitive to changes close to this boundary. In Figure 3 we plotted the Hausdorff distance d_H respectively the L_1-distance d_1 with respect to the noise level δ. The figure confirms, what we already recognized in Figure 2, that the quality of the identified inclusion Σ_α^δ improves with decreasing noise level. Both measures, the Hausdorff distance and the L_1-distance, are decreasing with the noise level δ.

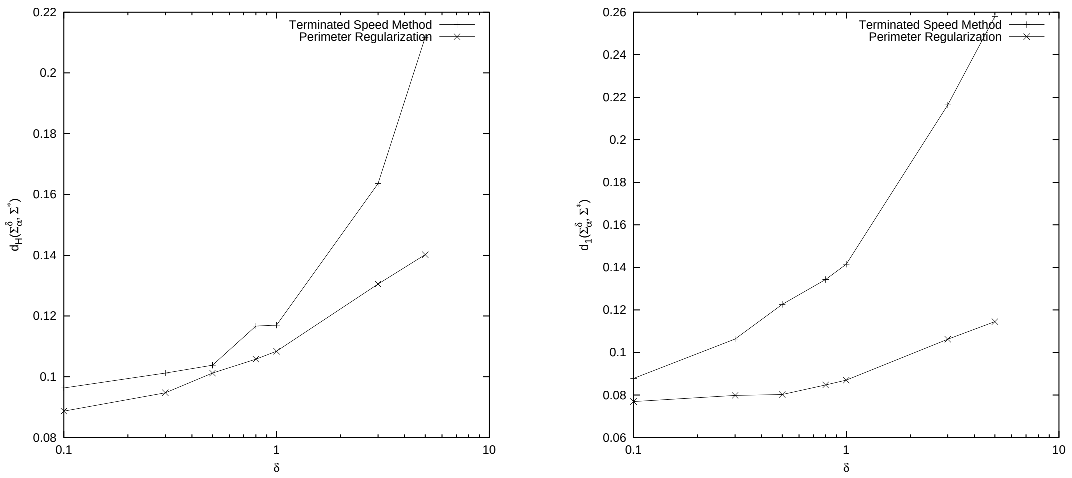

(a) Hausdorff distance $d_H(\Sigma_\alpha^\delta, \Sigma^*)$

(b) L_1-distance $d_1(\Sigma_\alpha^\delta, \Sigma^*)$

Figure 3: Ellipse: Convergence in Hausdorff- and L_1-distance versus noise δ

4.2 Sharp Ellipse

In the second test example the inclusion is as well an ellipse but with large respect ratio 6.

$$\Sigma^* = \left\{ (x,y) \mid \left(\frac{x}{0.6}\right)^2 + \left(\frac{y-0.1}{0.1}\right)^2 = 1 \right\}$$

The large respect ratio causes a rather large curvature which is a challenge for the PDE solver. Also the inverse solver suffers from this large curvature. This time we discretize the PDE (3.7) and the Hamilton-Jacobi equation (3.1) by a 513x513 grid in order to obtain a better resolution of the geometry. Only noise levels above $\delta \geq 1\%$ were done on a 257x257 grid.

Note that due to the large respect ratio of the ellipse for a 257x257 grid there are only a few grid points in the inclusion, which is a bit dangerous for the immersed interface discretization. As

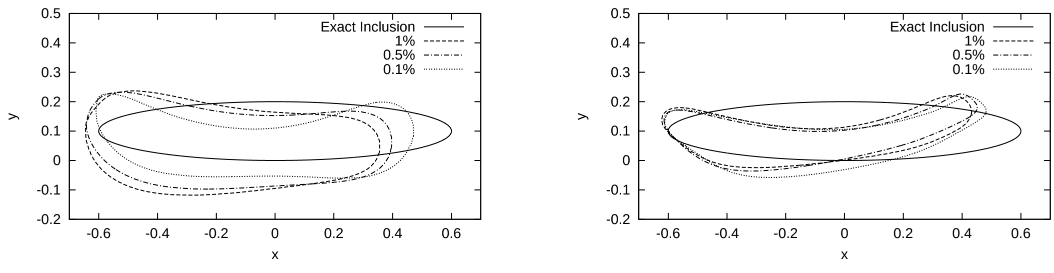

(a) Terminated Speed Method

(b) Perimeter Regularization

Figure 4: Sharp Ellipse: Identified inclusion for $\delta = 5, 1, 0.1\%$

before we present in Figure 4 the reconstructed inclusions for the noise levels $\delta = 5, 1, 0.1\,\%$ as well as the exact shape Σ^* for both, the terminated speed method and the perimeter regularization. Also here the reconstruction improves with decreasing noise. Nonetheless the reconstruction is still of poor quality for the finest noise level. The length and the width of the ellipse is almost correct but the curvature at the sharp radius is completely far off for the terminated speed method whereas the identified shape by the perimeter regularization gets too narrow. One may expect that for high curvature the reconstructed shape will not be very accurate, but surprisingly now the part of the interface with small curvature that is close to the Neumann boundary with constant load is far off the exact solution. For the same reason as for the ellipse with moderate respect ratio the reconstruction close to the Dirichlet boundary is of poor quality.

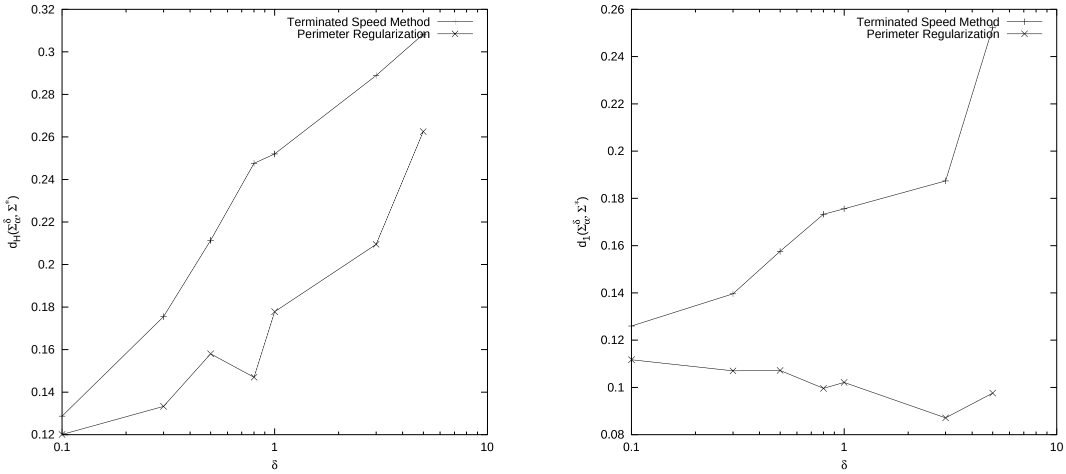

(a) Hausdorff distance $d_H(\Sigma_\alpha^\delta, \Sigma^*)$

(b) L_1-distance $d_1(\Sigma_\alpha^\delta, \Sigma^*)$

Figure 5: Sharp Ellipse: Convergence in Hausdorff- and L_1-distance versus noise δ

Despite the poor quality of the reconstruction in Figure 4 the error of the reconstructions in the Hausdorff distance decreases, as seen in Figure 5, with the noise level. This is again in accordance with our theory about the perimeter regularization and confirms the terminated speed method. For the perimeter regularization the L_1-distance seems to increase but this is not in contradiction to the theory developed before which is only valid for the Hausdorff distance d_H.

4.3 Star Shaped

Up to now all test examples where convex which is usually a quite nice property. In order to test a non-convex shape our third example is a star shaped inclusion.

$$\Sigma = \Big\{(x,y) \,|\quad x^2 + (y-0.1)^2 = \big(0.2 + 0.1 * \exp^{1.4*\cos(3*\kappa-2)+0.4*\sin\kappa}\big)^2, \quad \kappa = \arctan\frac{x}{y-0.1}\Big\}$$

The star shaped inclusion itself has again a quite large curvature and additionally the curvature is changing sign. So we can expect that this test example is quite hard for the algorithm. Especially from the last two examples we can not expect reconstructions of high quality in presence of noise.

For the discretization of the PDE (3.7) and the Hamilton-Jacobi equation (3.1) we chose a 257x257 grid.

As expected we observe in Figure 6 that the reconstructions get very poor, for both the perimeter regularization and the terminated speed method. Even worse Figure 7 indicates that the perimeter regularization is not converging which would contradict the theory. Fortunately we are so far off the solution that we can argue that the result do not contradict the theory which is only a local result. Despite this negative result one must be aware of the fact that the inclusion

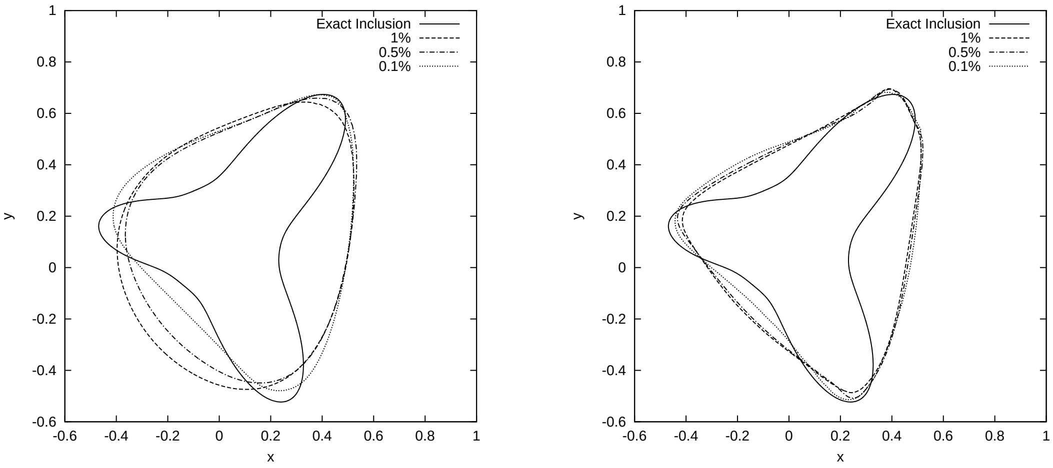

(a) Terminated Speed Method

(b) Perimeter Regularization

Figure 6: Star Shaped: Identified inclusion for $\delta = 5, 1, 0.1\%$

detection problem from a single boundary measurement is probably severely ill-posed, so we could not expect much better reconstructions.

We finally remark that even for visually poor reconstructions (cf. Figure 6) and increasing Hausdorff- and L_1-distance with decreasing noise level, the reconstruction is improved locally at the three arms of the star. The curvature of the reconstructed inclusion starts to change sign, too, when the noise is small enough. Hence, one would expect much better reconstructions for significantly lower noise levels, which seems to be unrealistic in practice. The only way to improve the quality of the reconstruction seems to be the use of multiple measurements (i.e., for measurements for different Neumann values). The application of level set methods in this case is an interesting and important topic for future research.

4.4 Two Circles

Our final example is probably the most challenging one. The inclusion consists of two circles, which can in principle be handled by the level set method as opposed to most classical shape reconstruction algorithms based on parameterizations. Again the PDE (3.7) and the Hamilton-Jacobi equation (3.1) are approximated by a 257x257 grid.

$$\Sigma = \{(x,y) \mid \begin{array}{l} (x+0.4)^2 + (y-0.4)^2 = 0.3^2 \text{ or} \\ (x-0.3)^2 + (y+0.3)^2 = 0.4^2 \} \end{array}$$

The identifiability result in Ben Ameur, Burger and Hackl [3] would theoretically allow to identify these multiply connected inclusions uniquely, but from the numerical tests in the previous examples it seems doubtful if this is possible in presence of noise. Indeed, the numerical results (cf. Figure 8) show that the initial domain does not split, but the algorithm shows at least a correct behavior, i.e., the Hausdorff distance between exact and reconstructed shape is decreasing with δ, and the shape seems to converge toward the correct inclusion.

For the terminated speed method we were not able to terminate according the termination criteria for small noise levels δ, it seems that the evolution got stuck in a local minimum. This indicates that also the reconstruction obtained with the perimeter regularization (looking similarly) might be a local minimum and not a global one. Figure 8 presents the calculated inclusions for

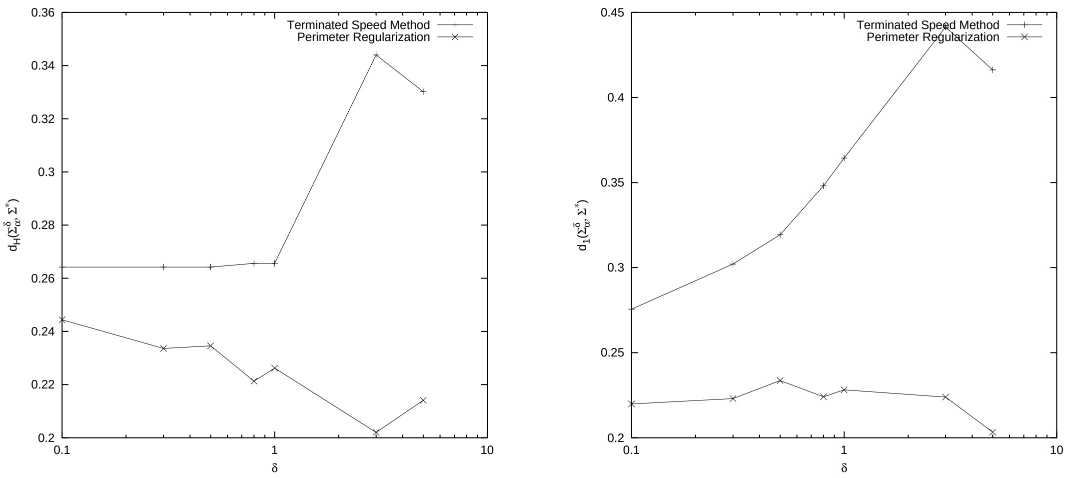

(a) Hausdorff distance $d_H(\hat{\Sigma}_\alpha^\delta, \hat{\Sigma})$ (b) L_1-distance $d_1(\hat{\Sigma}_\alpha^\delta, \hat{\Sigma})$

Figure 7: Star Shaped: Convergence in Hausdorff- and L_1-distance versus noise δ

noise levels $\delta = 1, 0.5, 0.1\,\%$ as well as the exact shape for the perimeter regularization. Visually, the reconstructions seem to get better when the noise δ reduces but still the components do not split into two components. As for the star shaped problem (Section 4.3) Figure 9 indicates that the Hausdorff distance for the perimeter regularization is increasing with the noise. This is either caused by getting stuck in a local minima or since the reconstructions are just too far from the exact solution to allow the application of the theoretical results.

5 Conclusions and Open Problems

We have presented a general approach to geometric inverse problems in linear elasticity, for which we also provided a convergent regularization method under very general geometric assumptions. Moreover, we have discussed the numerical solution of these inverse problems using the level set method, which allows to consider general shapes and does not rely on any parameterization.

The numerical results obtained for the anti-planar case are encouraging for future research. Especially an extension to more than one set of boundary measurements seems to be interesting. From related problems like impedance tomography and inverse scattering with full measurements (Dirichlet to Neumann map) it is well-known that the two-dimensional problem is not overdetermined, whereas the three-dimensional one is. Hence, a possible application of the inclusion detection problem to the general three-dimensional case (with full measurements) , which also is of importance in practice, may produce better results.

For the terminated speed method an analysis is still missing but the numerical results compared to the yet theoretically analyzed perimeter regularization give a good evidence to proceed with analyzing this method.

Moreover, many theoretical questions related to the solution by the level set method are still open, such as the well-posedness of this evolution and its regularizing properties. In particular for regular shapes there is some hope that we might apply local stability results obtained in Ben Ameur, Burger and Hackl [3] to obtain a convergence rate of the level set evolution, since the evolution uses exactly a path determined by the shape derivative, to which the stability estimates can be applied.

Analysis and computation is still open in the three-dimensional case, but we hope to obtain

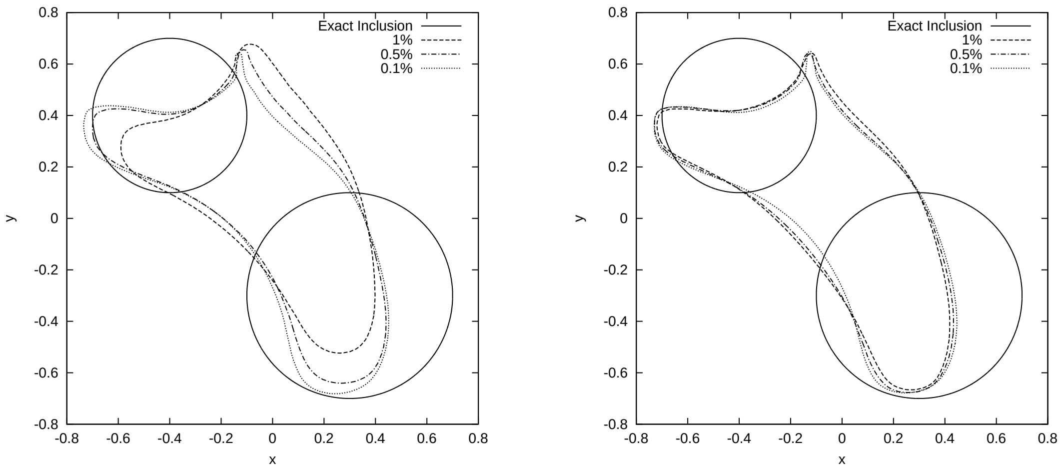

(a) Terminated Speed Method

(b) Perimeter Regularization

Figure 8: Two circle: Identified inclusion for $\delta = 1, 0.5, 0.1\%$

stability results in a similar way as for the two-dimensional planar case. Moreover, analogous questions are still open for thermo-elasticity, where the structural mechanics problems is coupled to a heat equation or for other types of material laws.

Acknowledgments

We thank Prof. Heinz W. Engl (University Linz) for stimulating this collaboration and for useful discussion. Moreover we thank Prof. Zhilin Li (UNC Charlotte) for providing a code for the solution of a Dirichlet problem for the Laplace equation by the immersed interface method, which we could use with some modifications for the solution of the direct problem in the anti-planar case. Financial support is acknowledged to the Austrian National Science Foundation FWF under grant SFB F 013 / 08 and P13478-INF.

References

[1] R.Acar, C.Vogel, *Analysis of bounded variation penalty methods for ill-posed problems* Inverse Problems **10** (1994), 1217-1229.

[2] B.Adalsteinsson, J.A.Sethian, *The fast construction of extension velocities in level set methods*,J. Comp. Phys. **148** (1999), 2-22.

[3] H.Ben Ameur, M.Burger, B.Hackl, *On some geometric inverse problems in linear elasticity*, Preprint(2003).

[4] K.Bryan, M.Vogelius *A uniqueness result concerning the identification of a collection of cracks from finitely many electrostatic boundary measurement* S.I.A.M.J.Math.Anal.**23** (1992).

[5] M.Burger, *A level set method for inverse problems*, Inverse Problems **17** (2001), 1327-1356.

[6] M.Burger, *A framework for the construction of level-set methods for shape optimization and reconstruction*, Interfaces and Free Boundaries **5** (2003), to appear.

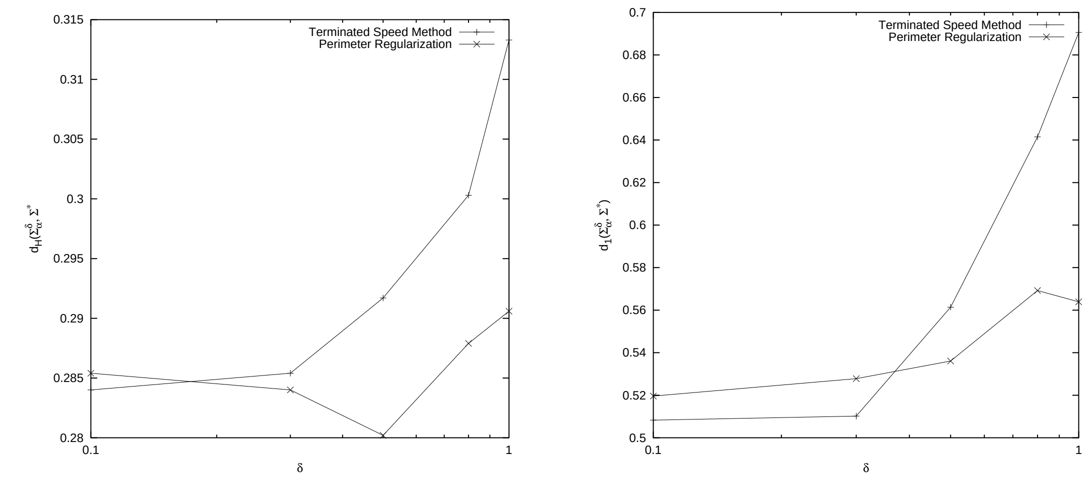

(a) Hausdorff distance $d_H(\Sigma_\alpha^\delta, \Sigma^*)$

(b) L_1-distance $d_1(\Sigma_\alpha^\delta, \Sigma^*)$

Figure 9: Two Circle: Convergence in Hausdorff- and L_1-distance versus noise δ

[7] J.W.Cahn, C.A.Handwerker, J.E.Taylor, *Geometric models of crystal growth*, Acta metall. mater. **40** (1992), 1443-1472.

[8] A.Chambolle, *A density result in two-dimensional linearized elasticity and applications*, Preprint (CEREMADE, Paris, 2001).

[9] D.Colton, R.Kress, *Inverse acoustic and electromagnetic scattering theory*, (J E Marsden & L Sirovich, Springer, (1998) second Edition).

[10] M.Crandall, H.Ishii, P.L.Lions, *User's guide to viscosity solutions of second order partial differential equations*, Bull. Am. Math. Soc. **27** (1992), 1-67.

[11] M.C.Delfour,J.-P.Zolésio *Shapes and geometries. Analysis, differential calculus, and optimization*, Advances in Design and Control. 4. Philadelphia, PA: SIAM. xvii, 482 p. (2001)

[12] A.Dervieux, B.Palmerio, *Une formule de Hadamard dans les problèmes d'identification de domaine*, C.R. Acad. Sci. Paris, serie I (1975), 1761-1764.

[13] H.W.Engl, M.Hanke, A Neubauer, *Regularization of Inverse Problems* (Kluwer, Dordrecht, 1996).

[14] H.W.Engl, K.Kunisch, A.Neubauer, *Convergence rates for Tikhonov regularisation of nonlinear ill-posed problems*, Inverse Problems **5** (1989), 523-540.

[15] H.Federer, *Geometric Measure Theory* (Springer, Berlin, Heidelberg, New York, 1969).

[16] A.Giacomini, *Generalization of Golab's Theorem and applications to fracture mechanics*, Math. Models Methods Appl. Sci. **12(9)** (2002), 1245-1267.

[17] F.Hettlich, W.Rundell *Iterative methods for the reconstraction of an inverse potential problems* Inverse problems, **12** (1996), 251-266.

[18] F.Hettlich, W.Rundell *Recovery of the support of source term in elliptic differential equation* Inverse problems, **13** (1997), 959-976.

[19] F.Hettlich, W.Rundell *The determination of a discontinuity in a conductivity from a single boundary measurement* Inverse Problems **14** (1998), 67-82.

[20] H.Huang, Z.Li, *Convergence analysis of the immersed interface method*, IMA Journal of Numerical Analysis, **19** (1999), 583-608.

[21] K.Ito, K.Kunisch, Z.Li, *Level-set function approach to an inverse interface problem*, Inverse Problems **17** (2001), 1225-1242.

[22] G.S.Jiang, D.Peng, *Weighted ENO schemes for Hamilton-Jacobi equations*, SIAM J. Sci. Comput., **21 (6)** (2000), 2126-2143.

[23] A.Kirsch *The detection of holes by elasto-static measurements* GAMM-Mitteilungen, Heft **1/2** (2000), 79-92.

[24] R.V.Kohn, M.Vogelius *Determining conductivity by boundary measurements; Interior results* Comm. in Pur Appl. Math., **38** (1985), 644-667.

[25] K.Kunisch, X.Pan *Estimation of interfaces from boundary measurements* SIAM J. Control Opt. **32** (1994), 1643-1674.

[26] R.LeVeque, Z.Li, *The immersed interface method for elliptic equations with discontinuous coefficients and singular sources*, SIAM J. Numer. Anal., **31** (1994), 1019-1044.

[27] Z.Li, *A fast iterative algorithm for elliptic interface problems*, SIAM J. Numer. Anal., **35 (1)** (1998), 230-254.

[28] Z.Li, *The immersed interface method using a finite element formulation*, Applied Numerical Mathematics, **27** (1998), 253-267.

[29] Z.Li, K.Ito, *Maximum principle preserving schmes for interface problems with discontinuous coefficients*, SIAM J. Sci. Comput., **23 (1)** (2001), 339-361.

[30] P.L.Lions, *Generalized solutions of Hamilton-Jacobi equations* (Pitman, Boston, London, Melbourne, 1982).

[31] A.Litman, D.Lesselier, F.Santosa, *Reconstruction of a two-dimensional binary obstacle by controlled evolution of a level-set*, Inverse Problems **14** (1998), 685-706.

[32] G.Dal Maso, R.Toader, *A model for the quasi-static growth of brittle fractures: existence and approximation results*, Arch. Rational Mech. Anal. **162** (2002), 101-135.

[33] J.M.Morel, S.Solimini, *Variational methods in image segmentation with 7 image processing experiments* (Birkhäuser, Basel, 1994).

[34] F.Murat, J.Simon, *Sur le contrôle par un domaine géometrique* (Publication du Laboratoire d'Analyse Numerique, Université de Paris VI, 1976).

[35] S.Osher, R.P.Fedkiw, *Level Set Methods and Dynamic Implicit Surfaces* (Springer, New York, 2002).

[36] S.Osher, F.Santosa, *Level set methods for optimization problems involving geometry and constraints I. Frequencies of a two-density inhomogeneous drum*, J. Comp. Phys. **171** (2001), 272-288.

[37] S.Osher, J.A.Sethian, *Fronts propagating with curvature-dependent speed: algorithms based on Hamilton–Jacobi formulations*, J. Comp. Phys. **79** (1988), 12–49.

[38] S.Osher, C.W.Shu, *Higher-Order Essentially Nonoscillatory Schemes for Hamilton-Jacobi Equations*, SIAM J. Numer. Anal., **28 (4)** (1991), 907-922.

[39] C.Ramananjaona, M.Lambert, D.Lesselier, *Shape inversion from TM and TE real data by controlled evolution of level sets*, Inverse Problems **17** (2001), 1585-1595.

[40] C.Ramananjaona, M.Lambert, D.Lesselier, J.P.Zolesio, *Shape reconstruction of buried obstacles by controlled evolution of a level set: from a min-max formulation to numerical experimentation*, Inverse Problems **17** (2001), 1087-1112.

[41] L.I.Rudin, S.Osher, E.Fatemi, *Nonlinear total variation based noise removal algorithms*, Physica D **60** (1992), 259-268.

[42] F.Santosa, *A level-set approach for inverse problems involving obstacles*, ESAIM: Control, Optimisation and Calculus of Variations **1** (1996), 17-33.

[43] T.I.Seidman, C.Vogel, *Well-posedness and convergence of some regularization methods for nonlinear ill posed problems*, Inverse Problems **5** (1989), 227-238.

[44] J.A.Sethian, *Level Set Methods and Fast Marching Methods* (Cambridge University Press, 2nd ed., Cambridge, 1999).

[45] J.A.Sethian, A.Wiegmann, *Structural boundary design via level set and immersed interface methods*, J. Comp. Phys. **163** (2000), 489-528.

[46] J.Sokolowski, J.P.Zolesio, *Introduction to Shape Optimization* (Springer, Berlin, Heidelberg, New York, 1992).

[47] U.Tautenhahn, *On the asymptotical regularization of nonlinear ill-posed problems*, Inverse Problems **10** (1994), 1405-1418.